HHS Public Access

Author manuscript

Oncogene. Author manuscript; available in PMC 2013 September 14.

Published in final edited form as:

Oncogene. 2013 March 14; 32(11): 1384–1395. doi:10.1038/onc.2012.163.

Nicotine/Cigarette-smoke Promotes Metastasis of Pancreatic Cancer Through α7nAChR-mediated MUC4 Up-regulation

Navneet Momi[1,4], **Moorthy P. Ponnusamy**[1,4], **Sukhwinder Kaur**[1], **Satyanarayana Rachagani**[1], **Sateesh S Kunigal**[3], **Srikumar Chellappan**[3], **Michel M Ouellette**[1,2], and **Surinder K Batra**[1,2]

[1]Department of Biochemistry and Molecular Biology, University of Nebraska Medical Center, Omaha, NE, U.S.A

[2]Eppley Institute for Research in Cancer and Allied Diseases, University of Nebraska Medical Center, Omaha, NE, U.S.A

[3]H. Lee Moffitt Cancer Center and Research Institute, Tampa, FL, USA

Abstract

Despite evidence that long-term smoking is the leading risk factor for pancreatic malignancies, the underlying mechanism(s) for cigarette-smoke (CS)-induced pancreatic cancer (PC) pathogenesis has not been well-established. Our previous studies revealed an aberrant expression of the MUC4 mucin in PC as compared to the normal pancreas and its association with cancer progression and metastasis. Interestingly, here we explore a potential link between MUC4 expression and smoking-mediated PC pathogenesis and report that both cigarette-smoke-extract (CSE) and nicotine, which is the major component of CS, significantly up-regulates MUC4 in PC cells. This nicotine-mediated MUC4 overexpression was via α7 subunit of nicotinic acetylcholine receptor (nAChR) stimulation and subsequent activation of the JAK2/STAT3 downstream signaling cascade in cooperation with the MEK/ERK1/2 pathway; this effect was blocked by the α7nAChR antagonists, α-bungarotoxin and mecamylamine, and by specific siRNA-mediated STAT3 inhibition. Additionally, we demonstrated that nicotine-mediated MUC4 up-regulation promotes the PC cell migration through the activation of the downstream effectors such as HER2, c-Src and FAK; this effect was attenuated by shRNA-mediated MUC4 abrogation, further implying that these nicotine-mediated pathological effects on PC cells are MUC4 dependent. Furthermore, the *in-vivo* studies demonstrated a dramatic increase in the mean pancreatic tumor weight [low-dose (100 mg/m^3 TSP), p=0.014; high-dose (247 mg/m^3 TSP), p=0.02] and significant tumor metastasis to various distant organs in the CS-exposed-mice, orthotopically implanted with luciferase-transfected PC cells, as compared to the sham-controls. Moreover, the CS-exposed mice had elevated levels of serum cotinine [low-dose, 155.88±35.96 ng/ml; high-dose, 216.25±29.95 ng/ml]

Correspondence: Surinder K. Batra, Ph.D., Department of Biochemistry and Molecular Biology, Eppley Institute for Research in Cancer and Allied Diseases, University of Nebraska Medical Center, Omaha, Nebraska, 68198-5870, U.S.A. Phone: 402-559-5455, Fax: 402-559-6650, sbatra@unmc.edu.

[4]These authors contributed equally to this work.

Disclosure of Potential Conflict of Interest

The authors declare no conflict of interest.

and increased MUC4, α7nAChR and pSTAT3 expression in the pancreatic tumor tissues. Altogether, our findings revealed for the first time that CS up-regulates the MUC4 mucin in PC via α7nAChR/JAK2/STAT3 downstream signaling cascade, thereby promoting metastasis of pancreatic cancer.

Keywords

MUC4; Mucin; Cigarette-smoke; Nicotine; Metastasis and Pancreatic Cancer

Introduction

Long-term smoking is among the most established risk factors for many cancers, including chronic pancreatitis and pancreatic cancer (PC) (1, 2). A large prospective study revealed that current smokers had a 2.5 times greater relative risk of developing PC compared to the non-smokers (3). Our previous investigations demonstrated that cigarette-smoke (CS) induces the expression of several genes involved in the exocrine function of the pancreas (4). With its complexity of constituents, CS causes morphological damage to the pancreas in multiple ways, which leads to an inflammatory response and alterations in the secretion of the pancreatic digestive enzymes (5).

Nicotine is the major addictive constituent of CS that induces modifications in the functional properties of cancer cells such as enhancing the rate of proliferation and angiogenesis (6, 7) at concentrations that are normally found in the blood-stream of smokers (10^{-8} M to 10^{-7} M) (6). Importantly, our previous studies showed high levels of nicotine and cotinine, which is a metabolic derivative of nicotine, in pancreatic tissues of CS-exposed animals (4, 8). Interestingly, the previous studies by other groups have demonstrated a direct association of colonic and gastric mucin secretion with nicotine uptake (9, 10).

Several studies have illustrated a strong correlation between the mucin expression and the development of cancer. Mucins are known to mediate their impact on tumor initiation and development via modulating cellular growth, differentiation, transformation, adhesion, invasion and immune surveillance (11–14). Our previous investigations have demonstrated a differential expression of a membrane bound mucin, MUC4, in pancreatic adenocarcinomas as compared to the normal pancreas (15). Furthermore, *de novo* expression of MUC4 was observed in early precancerous pancreatic intraepithelial neoplasias (PanINs) and its expression was increased progressively with the development of PC (16). Moreover, using the MUC4-knockdown and overexpression in the PC cell models, we have shown that MUC4 potentiates pancreatic tumor cell growth and metastasis by altering the behavioral properties of the cancer cells (17–19). Recently, our lab investigations have also demonstrated that MUC4 confers a resistance to anti-cancer agent gemcitabine in PC cells, hence rendering the current therapeutic regimens ineffective (20, 21).

Usually, PC patients have a mortality rate of nearly 100% and long-term exposure to cigarette-smoke is one of the several factors that contributes to this high rate (22). Therefore, a better understanding of the tobacco-smoking-mediated PC pathogenesis would lead to the

identification of potential molecular targets and is likely to improve the prospect of designing effective therapies to combat this lethal malignancy.

The current study establishes a novel link between the nicotine/CS-exposure and MUC4 overexpression in PC via the α7nAChR/JAK2/STAT3 downstream signaling cascade in cooperation with the MEK/ERK1/2 pathway. Importantly, the study illustrate that smoking increases the metastasis of pancreatic cancer through MUC4-mediated activation of the various downstream effectors such as FAK, HER2 and c-Src. Overall, our findings unfold new perspectives on the foundation of smoking-induced PC pathogenesis.

Results

Cigarette-smoke and nicotine up-regulates MUC4 expression in PC cells

Western blot analysis showed a progressive increase in the MUC4 expression in the cells treated with CSE in a dose-dependent manner from 10μl–200μl (Figure 1A). Interestingly, a progressive increase in MUC4 expression was also observed in a time dependent manner (4hrs, 8hrs and 24hrs), upon treatment with the major component of CS, nicotine (5μM) (Figure 1B). The CD18/HPAF cells, treated with different doses of nicotine (1μM, 5μM) for 24hrs time-point, also showed a dramatic increase in the MUC4 expression in a dose-dependent manner both at the protein level (~3 fold increase with the highest dose) and at the mRNA level (~2 fold increase with the highest dose) as compared to the untreated cells (Figure 1C). The confocal analysis confirmed the up-regulation of MUC4 expression in CD18/HPAF cells with nicotine treatment (1μM) as compared to the untreated cells (Figure 1C). Similar results were also observed in other PC cells, FG/Colo357 and Capan1 (Supplementary Figure 1A). Quite significantly, nicotine induced the MUC4 expression in the CD18/HPAF-SF PC cells that expresses MUC4 at undetectable levels under normal conditions (23), with treatment at concentrations as low as 0.1μM as compared to the untreated cells and it progressively increased with nicotine treatment in a dose-dependent manner, hence, demonstrating a more pronounced effect of nicotine on MUC4 expression (Figure 1D). However, no induction of MUC4 was observed in HPDE cells, the normal pancreatic epithelial cells that are negative for MUC4 expression under normal physiological conditions (Supplementary Figure 1B).

Nicotine stimulates the α7 subunit of nicotinic acetylcholine receptor in PC cells

With plentiful experimental evidences stating that nicotine exerts its cellular functions through nAChRs (24), in order to delineate the underlying regulatory mechanism(s) for the nicotine-induced MUC4 up-regulation, we investigated the expression levels of various nicotine receptor subunits, α5nAchR (53kDa), α7nAchR (55kDa) and α9nAchR (55kDa), in our PC cell models. Previous study has shown that α7 is the main nAChR subunit that mediates the proliferative effects of nicotine in cancer cells (25). Interestingly, the current study also demonstrated the stimulation of the α7nAChR subunit in the nicotine-treated CD18/HPAF-SF cells as compared to the untreated cells (Figure 1D); however, no change in the expression levels of the other receptor subunits was observed. Similarly, stimulation of α7nAChR subunit was also observed in CD18/HPAF (Figure 1E) and Capan1 cells (Supplementary Figure 2A), on nicotine treatment. Furthermore, treatment with the

α7nAChR subunit antagonist, α-bungarotoxin (α-BTX), demonstrated a down-regulation in the nicotine-induced MUC4 expression along with the decreased expression levels of α7nAChR subunit in CD18/HPAF (Figure 1E) and Capan1 cells (Supplementary Figure 2A). Similar results were also observed when treated with another α7nAChR subunit antagonist, mecamylamine (MAA) (Supplementary Figure 2A, Supplementary Figure 2B), with an overall confirmation of the role of α7nAChR subunit in mediating the MUC4 up-regulation in PC cells.

Nicotine induces α7nAChR subunit-mediated activation of the JAK2-STAT3 pathway in PC cells

Further, detailed studies were performed to elucidate the α7nAChR-mediated downstream signaling cascade leading to the MUC4 up-regulation. A dose-dependent treatment with nicotine showed a progressive increase in the phosphorylation of STAT3 (pY705) in the CD18/HPAF-SF cells (Figure 2A). The 1μM nicotine treatment showed an increased expression of pJAK2 and an enhanced activation of STAT3 (pY705) in CD18/HPAF cells (Figure 2B), which was significantly abrogated on treatment with α-BTX in CD18/HPAF cells, however, no change was observed in the total STAT3 expression (Figure 2B). Furthermore, the transient knockdown of STAT3 in CD18/HPAF cells via STAT3 specific siRNA resulted in significant down-regulation of nicotine-induced MUC4 as compared to scrambled vector-transfected CD18/HPAF cells (Figure 2C). It has been demonstrated that activation of another phosphorylation site of STAT3 (pS727) through Ras/Raf/MEK/ERK signaling cascade up-regulates the cytoplasmic concentration of STAT3 and is also known to increase the DNA-binding (26, 27). Interestingly, in our present studies nicotine treatment showed an increase in ERK1/2 activation in the CD18/HPAF cells (Figure 2D). Furthermore, treatment with an ERK inhibitor, UO126, demonstrated a down-regulation in nicotine-induced MUC4 expression along with reduced levels of both tSTAT3 and nicotine-induced pSTAT3 (pS727) (Figure 2E). Hence, the studies revealed a cooperation of the Ras/Raf/MEK/ERK and JAK2/STAT3 pathways downstream to α7nAChR as demonstrated in the previous studies with oral keratinocytes (28).

Nicotine-induced MUC4 increases the migratory potential of the PC cells

To assess the pathological impact of nicotine-induced MUC4 on the functional properties of PC cells, a wound healing assay in parallel with confocal analysis was performed with nicotine-treated CD18/HPAF cells. The level of wound recovery was higher in nicotine-treated CD18/HPAF cells in comparison to the untreated cells (Figure 3A). Similar results were also observed in Capan1 cells (Supplementary Figure 3A). Furthermore, the confocal studies demonstrated an increase in the MUC4 expression (Green; FITC) in CD18/HPAF cells upon nicotine treatment in a dose-dependent manner (0.1μM, 1μM, 5μM) for 24hrs (Figure 3A).

Nicotine increases the HER2, c-Src and FAK activation in the PC cells

Our previous studies demonstrated that MUC4 mucin interacts with and stabilizes the HER2 oncoprotein in PC cells (29). Interestingly, in the current study, the 1μM nicotine treatment showed a significant increase in the total HER2 expression as well as an increase in the phosphorylation of the HER2(pY1248) (Figure 3B). The immunofluorescence studies

further confirmed the up-regulation of the HER2 expression, and revealed its co-localization with MUC4 in the nicotine-treated CD18/HPAF cells as compared to untreated cells (Figure 3B). Importantly, the nicotine treatment (1μM) also showed increased levels of a cytoplasmic protein, c-Src, which is known to have tyrosine-specific protein kinase activity (Figure 3B). Moreover, the current study illustrated that the nicotine treatment resulted in increased FAK phosphorylation (pY925) in CD18/HPAF cells (Figure 3B), CD18/HPAF-SF cells (Figure 3C) and Capan1 cells (Supplementary Figure 3B), however, no change was observed in the total FAK expression. It is well known that FAK as well as the FAK-mediated signaling network plays an important role in cancer metastasis and that it is a downstream effector protein in HER2 signaling (30).

Nicotine-induced MUC4 as the major cause for increased migratory potential of PC cells

Previously, our investigations have shown that inhibition of MUC4 expression suppresses the pancreatic tumor metastasis (17, 19). Hence, to investigate the specific role of nicotine-mediated-MUC4 in imparting an enhanced migratory potential to the PC cells, the wound healing assay was performed using the MUC4 knockdown CD18/HPAF cells (CD18/HPAF/shMUC4) under nicotine treatment. A comparison was made with the scrambled-vector transfected CD18/HPAF cells (CD18/HPAF/scr). Further, the confocal analysis was carried out to assess the correlation between the nicotine-induced MUC4 expression and the change in the migration potential of the cells. Both confocal analysis and western blot analysis showed reduced expression of MUC4 in CD18/HPAF/shMUC4 cells as compared to the CD18/HPAF/scr cells (Figure 4A). Moreover, CD18/HPAF/scr cells showed an increase in the migration potential with nicotine treatment, however, no variation was observed in case of CD18/HPAF/shMUC4 cells (Figure 4A). The expression levels of the downstream effectors of MUC4 such as HER2, pHER2 and pFAK were analyzed in the MUC4 knockdown cells under nicotine treatment. 1μM nicotine treatment up-regulated the MUC4 expression, leading to an increased expression of pFAK in CD18/HPAF/scr cells compared to the CD18/HPAF/shMUC4 cells (Figure 4B). We also observed comparatively higher fold of up-regulation in HER2 and pHER2 expression in CD18/HPAF/scr cells as compared to the CD18/HPAF/shMUC4 cells (Figure 4B). Similar results were also observed in Capan1 cells (Supplementary Figure 3C).

Cigarette-smoke exposure increases the pancreatic tumor weight and potentiates tumor metastasis

Further, the effect of cigarette-smoke exposure on the PC tumorogenesis was evaluated *in-vivo*. The whole-body imaging of the immunodeficient mice, orthotopically implanted with CD18/HPAF-luciferase cells, after six weeks of CS exposure, showed a significant increase in the tumor metastasis in animal groups exposed to both low and high doses as compared to the sham controls (Figure 5A). Moreover, the mean tumor size was found to be progressively increased in the smoke-exposed animals as compared to the sham controls (low-dose, p=0.014; high-dose, p=0.02) (Figure 5A). Interestingly, a significantly increased tumor metastasis was observed in both the CS-exposed mice groups. A very significant increase of tumor metastasis was observed in the liver (n=6/7; p=0.0041) and stomach (n=5/7; p=0.0082) of mice exposed to high-dose as compared to the sham control (liver, n=1/7; stomach, n=0/7). The other organs that showed significant metastasis in high-dose-

exposed mice were the spleen (p=0.0317) and mesenteric lymph nodes (p=0.0317). In low-dose-exposed mice, significant metastasis occurred in the liver (p=0.0317), spleen (p=0.0317) and mesenteric lymph nodes (p=0.0317). Additionally, metastasis to the peritoneal wall (p=0.0781) and the kidneys (p=0.0781) in the case of high-dose-exposed mice, and to the stomach (p=0.0781) in the case of low-dose-exposed mice (Figure 5B), was also observed.

Expression of MUC4, α7nAChR and pSTAT3 in the xenograft pancreatic tumor tissues after the cigarette-smoke exposure

The averaged cotinine levels ± SEM were 155.88±35.96ng/ml and 216.25±29.95ng/ml for low-dose-exposed and high-dose-exposed animals, respectively. The values were comparable to the serum cotinine levels in immunocompromised mice as seen in the studies by Wong et al (31). The xenograft mean pancreatic tumor size was increased both in low-dose-exposed (p=0.014) and high-dose-exposed animals (p=0.02) as compared to the sham controls (Figure 6A). To evaluate the effect of CS-exposure on the histomorphological alterations of the pancreas and various other organs with tumor metastasis, such as the spleen, liver, stomach and kidney, the tissues were fixed, the sections were cut and stained with Haematoxylin and Eosin (H&E). The H&E staining showed morphological alterations clearly differentiating the cancer tissues from the normal tissues (Figure 6A). The MUC4 expression showed progressive increase from sham controls to CS-exposed mice groups (Figure 6B), demonstrating the correlation between the MUC4 expression and CS-exposure. Moreover, the expression levels of the α7nAChR subunit and pSTAT3 (Y705) were up-regulated in the CS-exposed mice as compared to the sham controls (Figure 6B).

Discussion

Our earlier studies have shown the specific and differential expression of MUC4 in pancreatic adenocarcinoma as compared with the normal pancreas or chronic pancreatitis (15). Here, in the current study, we aim to investigate the effect of nicotine/CS on PC pathogenesis and to explore the potential link between nicotine/cigarette-smoke-exposure and MUC4 expression in PC. Interestingly, the CSE demonstrated a progressive increase in the MUC4 expression in the PC cells. Furthermore, our *in-vivo* studies also revealed a progressive increase of MUC4 expression in the pancreatic tissues of the CS-exposed mice as compared to the sham controls, hence validating our *in-vitro* observations. Previous studies have shown that the major component of cigarette-smoke, nicotine, which is not carcinogenic by itself, has been associated with PC carcinogenesis by increasing the pancreatic protein synthesis in isolated acini (32). Importantly, in the current study, a significant MUC4 up-regulation in PC cells upon treatment with nicotine itself showed that this component of tobacco-smoke is indeed self-sufficient to contribute to PC pathogenesis. However, the normal pancreatic epithelial cells, that normally do not express MUC4, showed no induction of MUC4 expression when treated with nicotine (Supplementary Figure 1B). These observations were in accordance with the literature demonstrating that smoking contributes more to the promoting than to the initiating phase of cancer (33).

Having seen a strong correlation between the nicotine/CS-exposure and MUC4 overexpression, we next aimed to elucidate the possible regulatory mechanism(s) behind the nicotine-mediated MUC4 induction and to illustrate the downstream signaling cascade. It is well known that nicotine imitates the action of a natural neurotransmitter called acetylcholine and by itself exerts its cellular functions through nAChRs (24). Recent studies have shown that α7 is the main nAChR subunit that mediates the proliferative effects of nicotine in cancer cells (25). In the present study, we also observed an up-regulation of the α7nAChR in the nicotine-treated PC cells. When the cells were treated with the α7nAChR antagonists, α-BTX and MAA, the expression levels of both MUC4 and the α7 nicotine receptor subunit decreased significantly, confirming the specificity of the α7nAChR subunit in nicotine-mediated MUC4 induction in PC cells. While these results seem compelling, the exact mechanism responsible for the apparent α7nAChR stimulation in context to nicotine remains unclear. Interestingly, in the present study we observed that the nicotine-induced MUC4 expression in PC cells was abrogated upon treatment with a calcium channel blocker, Nifedipine (Supplementary figure 2C). It is known that Ca^{2+} usually serves as a second messenger in the nicotine-mediated signaling pathways. In support of this theory, a study indicated that NNK-mediated activation of α7nAChR raises the Ca^{2+} influx into lung cells resulting in membrane depolarization and subsequent activation of voltage-gated Ca^{2+} channels (34). Moreover, nAChRs, being the ligand-gated cationic channels, are highly permeable to calcium ions (35). This increased Ca^{2+} influx through both the nAChRs and Ca^{2+} channels eventually lead to nAChR up-regulation, suggesting that there might be a positive feedback loop associated with the nicotine-induced nAChR signaling (36).

Various studies have demonstrated that nicotine activates multiple transcription factors such as E2F1 and $NF_{\kappa}B$ (37, 38). Notably, the nicotine-mediated pathological effects in several malignancies are mediated via pathways governed by STATs, a signal transducer and activator of transcription, as demonstrated by several reports such as in head and neck squamous cell carcinoma (28, 39) and bladder cancer (40). Recently, Chen *et al.* demonstrated that nicotine strongly activates STAT3, leading to cell cycle perturbations and chemoresistance in human bladder cancer cells (41). Studies have also shown a cooperation of the Ras/Raf/MEK/ERK and JAK2/STAT3 pathways downstream of α7nAChR in oral keratinocytes leading to alterations in gene expression due to transactivation of STAT3. The stepwise activation of Ras/Raf/MEK/ERK up-regulates the cytoplasmic concentration of STAT3 and is also known to induce the phosphorylation of STAT3 (pS727). Some reports also indicate a correlation of STAT3 serine phosphorylation with increased DNA-binding (26, 27). The activation of tyrosine kinase JAK2, on the other hand, potentiates the phosphorylation of STAT3 (pY705) leading to the STAT3-dimerization with subsequent translocation to the nucleus to alter the expression of various genes (28). Interestingly, in the present study, the nicotine-induced MUC4 up-regulation was attributed to STAT3 activation through both the pathways mediated by JAK2 (pSTAT3-Y705) and ERK1/2 (pSTAT3-S727). Moreover, in the *in-vivo* studies, the expression levels of the α7nAChR subunit and pSTAT3 (pY705) were significantly enhanced in the CS-exposed animals as compared to the sham controls.

Several studies have shown that STAT3 activation plays a profound role in the aberrant gene expression, including the mucin overexpression. Andoh *et al*. showed the STAT3 phosphorylation in HT-29 colonic epithelial cells significantly increasing the mRNA expression of membrane-bound mucins (MUC1, MUC3, and MUC4) (42). In gastric cancer, an association between STAT3 activation and MUC4 up-regulation has been shown where STAT3 binds to a cis-element on the MUC4 promoter (43). In a recent study by the same group, high expression levels of Muc4 were found in gastric tumors developed in gp130 (Y757F/Y757F) mice, with hyper-activated STAT3 (44). In the present study, we observed attenuation of MUC4 expression in the PC cells with transient knockdown of STAT3. We also observed a decreased activation of STAT3 in PC cells after treating them with α7nAChR-antagonists, further confirming that the STAT3 activation is downstream to α7nAChR. Collectively, these results strongly supported the relevance of STAT3 in MUC4 regulation and provided clear evidence that the α7nAChR/JAK2/STAT3 signaling cascade, in association with the Ras/Raf/MEK/ERK1/2-mediated pathway, is the possible mechanism behind the nicotine-induced MUC4 up-regulation in PC. Various other studies have established the role of another signal transduction regulator, STAT1, in tobacco-related carcinogenesis (45, 46). Moreover, previous studies in our lab have shown that the induction of MUC4 by IFNγ occurs via a pathway involving the up-regulation of STAT1 in PC cells (47, 48). Therefore, exploring the role of the STAT1 signal transduction regulator in CS-mediated PC pathogenesis would be an interesting aspect for future studies.

With regard to the tumorigenic potential of MUC4 in PC (19), in the current study, we further analyzed the effect of the nicotine-mediated MUC4 up-regulation on the functional properties of the PC cells. Our results revealed that the nicotine-mediated up-regulation of the MUC4 mucin potentiates the migration of the PC cells. The *in-vivo* studies also demonstrated the CS-exposure-mediated significant pancreatic tumor metastasis to various distant organs such as peritoneal wall, mesenteric-lymph-nodes, liver, spleen, kidney and stomach. Further, to confirm that the nicotine-mediated effects are MUC4-dependent and not due to the effect of nicotine itself, studies were performed by knockdown of MUC4 in PC cells followed by the nicotine treatment. It was observed that nicotine fails to increase the migratory potential of the PC cells in the absence of MUC4, thus, clearly demonstrating that nicotine-induced MUC4 is the major contributing factor for the augmented migration of the PC cells.

Having seen the stimulatory effect of nicotine/CS on the PC cells' migration, further, a detailed elucidation was made to access the pathways downstream of nicotine-induced-MUC4, responsible for the migratory potential of the PC cells. This important phenotypic change may either directly result from the MUC4-elicited changes in the actin reorganization due to steric hindrance caused by its large size or indirectly through HER2-mediated pathways. The interaction of MUC4 with HER2 in PC cells was shown in our previous studies and evidence was provided that this interaction stabilizes HER2 (29). It is well known that FAK, as well as the FAK-mediated signaling network plays an important role in cancer metastasis (30). Recently, our group showed that MUC4 plays a role in ovarian cancer cell motility, partly by altering the actin re-arrangements and potentiating HER2 downstream signaling through FAK activation (49). Interestingly, in the present

study, nicotine robustly increased the total-HER2 expression levels in PC cells and also leads to its activation by stabilizing pHER2 (pY1248). Additionally, the FAK activation (pY925) was also observed in PC cells upon nicotine treatment.

It is known that elevated Src activity results in the activation of integrin and FAK mediated signaling, which causes the suppression of cell–cell adhesion (50). Vadlamudi *et al* have shown that HER2 signaling selectively activates c-Src and FAK, leading to an increased cellular motility in breast cancer (51). This suggests that HER2, coupled with activated c-Src and FAK, plays an important role in aggravating the migratory potential of the cancer cells. In the current study, nicotine also induces the activation of this cytoplasmic protein, c-Src, in PC cells, based on which we speculate that this might be an alternate downstream signaling pathway. Finally, in the MUC4 knockdown studies, we observed that the nicotine induced high levels of MUC4 in scr-vector-transfected PC cells leading to increased expression levels of pFAK, HER2 and pHER2. However, in the shMUC4-transfected PC cells, the low levels of MUC4 resulted in not much of an increase in the HER, pHER2 and pFAK expression patterns. These findings in the current study clearly reveal that HER2, FAK and c-Src are the downstream effectors of MUC4 involved in the nicotine-induced increase in the migration potential of PC cells.

In conclusion, our data highlights a novel finding that CS/nicotine up-regulates the MUC4 mucin expression in PC through the α7nAchR-mediated JAK2/STAT3 signaling cascade in cooperation with Ras/Raf/MEK/ERK1/2 mediated pathway, significantly aggravating the PC metastasis. The study also unveils that this nicotine-mediated effect is through various MUC4 downstream effectors, such as FAK, HER2 and c-Src (Figure 7). Overall, our findings provide a significant mechanistic and functional insight into CS-induced PC pathogenesis and support the concept that MUC4 is a relevant therapeutic target for this lethal malignancy. In the future, it will be of interest to validate these observations in PC patients' samples having a positive history of cigarette-smoking, to support the pathogenic relevance of MUC4 with the acquisition of smoking-induced PC pathogenesis.

Materials and Methods

Preparations of cigarette-smoke extract (CSE)

CSE was prepared by allowing the flow of cigarette-smoke directly to the medium in a glass flask with a side-stream smoke exposure system. Two 3R4F filtered reference cigarettes (Tobacco and Health Research Institute, University of Kentucky) were used to generate cigarette-smoke. The protocol variables attempt to mimic a standardized human smoking pattern. Each cigarette was smoked under rigid conditions of 1 puff (35 ml) volume for a 2 sec duration/min over a period of 8 min, delivering approximately 0.8 mg of nicotine/ cigarette.

Cell line model

The cell lines used were CD18/HPAF, Capan1 and FG/Colo357, representing a well-differentiated stage of PC (17, 19). Additionally, in order to see a more pronounced effect of nicotine on MUC4 regulation, a serum-free (SF)-adapted derivative of CD18/HPAF cells

(CD18/HPAF-SF) was used, that expresses undetectable endogenous MUC4, while being cultured in DMEM/F12 media without serum (48). To see the effect of nicotine on the normal pancreatic epithelia, the human pancreatic ductal epithelial (HPDE) cells were used. The stable MUC4-knockdown PC cells (CD18/HPAF/shMUC4 and Capan1/shMUC4) as well as their stable scrambled-vector control cells (CD18/HPAF/scr and Capan1/scr) were generated by infecting parental cells with retroviral particles produced from plasmid pSUPER-retro puro.shMUC4 or pSUPER-retro.scr (17). For the *in-vivo* imaging studies, CD18/HPAF cells were transduced with retroviral particles produced from plasmid pMSCV-IRES-Luciferase (Addgene, MA) and positive clones for the presence of luciferase activity were screened and isolated.

Treatment with CSE, nicotine, α7nAChR subunit antagonists and ERK inhibitor

Cells were seeded at a density of 1×10^6 cells/well in a six-well plate and treated with different doses of CSE (10μl–200μl). For treatment with nicotine (purchased from Sigma), cells were seeded in similar fashion and treated in a dose-dependent manner for 24hrs (1μM–5μM) as well as in a time-dependent manner with 5μM nicotine for (4hrs, 8hrs and 24hrs). The CD18/HPAF-SF cells were seeded at a density of 2×10^6 cells/well in a six-well plate and treated in a dose-dependent manner for 24hrs (0.1μM, 1μM). For inhibitor studies, the cells were treated with α7 subunit of nicotine receptor antagonists, α-bungarotoxin (α-BTX) (1μM) and mecamylamine (MAA) (1μM), and ERK inhibitor (UO126) (1μM), 1hr prior to the nicotine treatment. All of the treatments were carried out with serum-free DMEM under dark conditions.

Western blotting analysis

The cell lysates preparation and Western blotting was done as per the standard procedures (19). For MUC4, the proteins (20μg) were resolved by electrophoresis on a 2% SDS-agarose gel under reducing conditions. For rest of the proteins, the 10%-SDS-PAGE was performed under similar conditions. Primary Antibodies used for the immunodetection were anti-MUC4 (8G7, 1:2500), anti-α9nAChR/anti-α5nAChR (gifted by Dr S. Chellappan, FL), anti-c-Src and anti-p-HER2(Y1248) (Upstate, San Francisco, CA). anti-STAT3, anti-ERK1/2, anti-FAK, anti-p-FAK(Y925) and anti-HER2 from Santa Crutz Biotechnology. anti-β-actin, anti-p-STAT3(S727) from Sigma, St Louis, MO, anti-α7nAChR, anti-p-JAK2(Y1007/1008) from Abcam and anti-p-STAT3(Y705), anti-p-ERK1/2 from Cell Signaling Technology Inc, MA. Resolved proteins were transferred on to the PVDF membrane and immunoblot assay was performed.

Reverse transcription-PCR

Total RNA was isolated from the cells and 2μg of total RNA was used for the reverse transcription using the first-strand cDNA synthesis kit (Perkin-Elmer) and oligo-d(T) primers. PCR was performed for MUC4 gene. The initial PCR activation step was at 94°C for four minutes, followed by the denaturation step at 94°C for one minute, primer-annealing step at 58°C for 30 seconds, extension step at 72°C for one minute and the final extension step at 72°C for ten minutes (19).

Wound healing assay

A total of 1×10^6 Capan1 cells/well and 70,000 CD18/HPAF cells/well were plated and grown asynchronously to 90% confluency in a six-well plate and a twelve-well plate, respectively. A scratch was made in three separate places in each well and treated with nicotine (0.1μM, 1μM and 5μM) for 24hrs. Images were taken at 10X magnification at 0hrs (t=0hrs) and 24hrs (t=Δhrs) time point. The area of wound was quantified by Java's Image J software

Immunofluorescence and confocal microscopy

CD18/HPAF/shMUC4 and CD18/HPAF/scr cells (70,000 cells/well) were plated onto the cover slip in each well of a twelve-well plate for immunostaining and treated with 1μM nicotine. On the same cover slips, the wound healing assay was performed. The immunostaining procedure was followed as per our previous methods (17, 49).

STAT3 knockdown using specific siRNA

A pool of three STAT3 specific siRNA oligos (Santa Cruz, CA) was transfected into CD18/HPAF cells by transient transfection using Lipofectamine 2000 reagent (Invitrogen, CA). After 48hrs of transfection, siSTAT3-transfected CD18/HPAF cells and scrambled siRNA-transfected CD18/HPAF cells were processed for protein extraction and Western blotting.

Cigarette-smoke exposure and whole body in-vivo imaging

Luciferase containing CD18/HPAF cells (5×10^5 cells/mice) were orthotopically implanted in the pancreas of 4–6 week old immunodeficient mice (19). One week after implantation, animals were exposed to cigarette-smoke, which was generated by smoking a 3R4F filtered reference cigarette. Mainstream and sidestream smoke was mixed with room air, conditioned, and drawn into the rodent exposure chamber (TE-10, Teague Enterprises, CA). The average total suspended particulate (TSP) matter was determined by filtering the air at a constant flow rate of 5L/min through a 0.3μm filter and determined by the change in its weight. The animals were randomized into three groups as sham controls (n=7), low-dose-exposed (n=7) and high-dose-exposed (n=7). Animals were exposed once every day for six weeks, to an average of 100 mg/m^3 TSP for the low-dose and 247 mg/m^3 TSP for the high-dose for 70mins. The group of sham-control animals was exposed to filtered air. After six weeks of exposure, whole body Luciferase bioluminescent images were taken using a Xenogen IVIS-100, following the intraperitoneal injection of D-luciferin substrate (Caliper Life sciences) (160μl/mice). Animals were sacrificed, primary tumor was resected and the presence of metastatic lesions in different organs was determined. Pancreatic tumors were excised and weighed. For protein extraction, pancreas was snap-frozen in liquid nitrogen followed by storage at −80°C.

Measurement of Cotinine levels in serum

The cotinine level were measured by competitive ELISA (Calbiotech) in serum obtained by incubating whole blood for 30min at 37°C, followed by centrifugation. Briefly, 10μl of standards, controls and serum samples from smoked and control mice were added in duplicates to anti-cotinine antibody coated plates, followed by the addition of 100μl of

Cotinine-HRP Enzyme Conjugate and 1hr incubation under dark conditions. After six washings with distilled water, the reaction was developed by adding 100μl of TMB substrate solution followed by 30min incubation at room temperature under dark conditions. Once the desired color was developed, the reaction was stopped by adding 50μl of 1M sulfuric acid. The plates were read at 450nm and data was analyzed using the SOFTMAX PRO software (Molecular Devices Corp, CA).

Histology and Immunohistochemistry

The resected tumors were fixed in 10% neutral-buffered formalin before processing into paraffin blocks. Tissue sections (5mm thick) were cut from the blocks and stained with H&E and with antibodies against α7nAChR (1:50 dilution, Abcam), pSTAT3 (Y705) (1:50 dilution, (Cell Signaling Technology) and MUC4 (8G7, 1:2500 dilution). The immunohistochemical staining was performed following our standardized procedure (19).

Supplementary Material

Refer to Web version on PubMed Central for supplementary material.

Acknowledgments

We thank Ms. Kristi L. Berger for editing the manuscript. The authors acknowledge the invaluable technical support from Mr. Erik Moore and Mrs. Kavita Mallya. We also thank Janice A. Tayor and James R. Talaska, the members of the confocal laser scanning microscope core facility at UNMC, for their support.

This work was, in part, supported by grants from the National Institutes of Health (RO1 CA133774, RO1 CA131944, RO1 CA78590, UO1 CA111294, P50 CA127297 and U54 CA163120)

References

1. Boyle P, Maisonneuve P, Bueno de MB, Ghadirian P, Howe GR, Zatonski W, et al. Cigarette smoking and pancreas cancer: a case control study of the search programme of the IARC. Int J Cancer. 1996; 67:63–71. [PubMed: 8690527]
2. Muscat JE, Stellman SD, Hoffmann D, Wynder EL. Smoking and pancreatic cancer in men and women. Cancer Epidemiol Biomarkers Prev. 1997; 6:15–19. [PubMed: 8993792]
3. Fuchs CS, Colditz GA, Stampfer MJ, Giovannucci EL, Hunter DJ, Rimm EB, et al. A prospective study of cigarette smoking and the risk of pancreatic cancer. Arch Intern Med. 1996; 156:2255–2260. [PubMed: 8885826]
4. Wittel UA, Singh AP, Henley BJ, Andrianifahanana M, Akhter MP, Cullen DM, et al. Cigarette smoke-induced differential expression of the genes involved in exocrine function of the rat pancreas. Pancreas. 2006; 33:364–370. [PubMed: 17079941]
5. Malfertheiner P, Schutte K. Smoking--a trigger for chronic inflammation and cancer development in the pancreas. Am J Gastroenterol. 2006; 101:160–162. [PubMed: 16405549]
6. Heeschen C, Jang JJ, Weis M, Pathak A, Kaji S, Hu RS, et al. Nicotine stimulates angiogenesis and promotes tumor growth and atherosclerosis. Nat Med. 2001; 7:833–839. [PubMed: 11433349]
7. Heeschen C, Weis M, Aicher A, Dimmeler S, Cooke JP. A novel angiogenic pathway mediated by non-neuronal nicotinic acetylcholine receptors. J Clin Invest. 2002; 110:527–536. [PubMed: 12189247]
8. Wittel UA, Pandey KK, Andrianifahanana M, Johansson SL, Cullen DM, Akhter MP, et al. Chronic pancreatic inflammation induced by environmental tobacco smoke inhalation in rats. Am J Gastroenterol. 2006; 101:148–159. [PubMed: 16405548]

9. Finnie IA, Campbell BJ, Taylor BA, Milton JD, Sadek SK, Yu LG, et al. Stimulation of colonic mucin synthesis by corticosteroids and nicotine. Clin Sci (Lond). 1996; 91:359–364. [PubMed: 8869420]
10. Luk IS, Ho J, Wong WM, Yuen ST, Luk CT, Cho CH. Influence of chronic nicotine intake and acute ethanol challenge on gastric mucus level and blood flow in rabbits. Digestion. 1994; 55:399–404. [PubMed: 7535712]
11. Chaturvedi P, Singh AP, Batra SK. Structure, evolution, and biology of the MUC4 mucin. FASEB J. 2008; 22:966–981. [PubMed: 18024835]
12. Rachagani S, Torres MP, Moniaux N, Batra SK. Current status of mucins in the diagnosis and therapy of cancer. Biofactors. 2009; 35:509–527. [PubMed: 19904814]
13. Kufe DW. Mucins in cancer: function, prognosis and therapy. Nat Rev Cancer. 2009; 9:874–885. [PubMed: 19935676]
14. Bafna S, Kaur S, Batra SK. Membrane-bound mucins: the mechanistic basis for alterations in the growth and survival of cancer cells. Oncogene. 2010; 29:2893–2904. [PubMed: 20348949]
15. Andrianifahanana M, Moniaux N, Schmied BM, Ringel J, Friess H, Hollingsworth MA, et al. Mucin (MUC) gene expression in human pancreatic adenocarcinoma and chronic pancreatitis: a potential role of MUC4 as a tumor marker of diagnostic significance. Clin Cancer Res. 2001; 7:4033–4040. [PubMed: 11751498]
16. Swartz MJ, Batra SK, Varshney GC, Hollingsworth MA, Yeo CJ, Cameron JL, et al. MUC4 expression increases progressively in pancreatic intraepithelial neoplasia. Am J Clin Pathol. 2002; 117:791–796. [PubMed: 12090430]
17. Chaturvedi P, Singh AP, Moniaux N, Senapati S, Chakraborty S, Meza JL, et al. MUC4 mucin potentiates pancreatic tumor cell proliferation, survival, and invasive properties and interferes with its interaction to extracellular matrix proteins. Mol Cancer Res. 2007; 5:309–320. [PubMed: 17406026]
18. Moniaux N, Chaturvedi P, Varshney GC, Meza JL, Rodriguez-Sierra JF, Aubert JP, et al. Human MUC4 mucin induces ultra-structural changes and tumorigenicity in pancreatic cancer cells. Br J Cancer. 2007; 97:345–357. [PubMed: 17595659]
19. Singh AP, Moniaux N, Chauhan SC, Meza JL, Batra SK. Inhibition of MUC4 expression suppresses pancreatic tumor cell growth and metastasis. Cancer Res. 2004; 64:622–630. [PubMed: 14744777]
20. Bafna S, Kaur S, Momi N, Batra SK. Pancreatic cancer cells resistance to gemcitabine: the role of MUC4 mucin. Br J Cancer. 2009; 101:1155–1161. [PubMed: 19738614]
21. Mimeault M, Johansson SL, Senapati S, Momi N, Chakraborty S, Batra SK. MUC4 down-regulation reverses chemoresistance of pancreatic cancer stem/progenitor cells and their progenies. Cancer Lett. 2010; 295:69–84. [PubMed: 20303649]
22. Lowenfels AB, Maisonneuve P. Risk factors for pancreatic cancer. J Cell Biochem. 2005; 95:649–656. [PubMed: 15849724]
23. Choudhury A, Singh RK, Moniaux N, El-Metwally TH, Aubert JP, Batra SK. Retinoic acid-dependent transforming growth factor-beta 2-mediated induction of MUC4 mucin expression in human pancreatic tumor cells follows retinoic acid receptor-alpha signaling pathway. J Biol Chem. 2000; 275:33929–33936. [PubMed: 10938282]
24. Lindstrom J, Schoepfer R, Whiting P. Molecular studies of the neuronal nicotinic acetylcholine receptor family. Mol Neurobiol. 1987; 1:281–337. [PubMed: 3077062]
25. Egleton RD, Brown KC, Dasgupta P. Nicotinic acetylcholine receptors in cancer: multiple roles in proliferation and inhibition of apoptosis. Trends Pharmacol Sci. 2008; 29:151–158. [PubMed: 18262664]
26. Ng J, Cantrell D. STAT3 is a serine kinase target in T lymphocytes. Interleukin 2 and T cell antigen receptor signals converge upon serine 727. J Biol Chem. 1997; 272:24542–24549. [PubMed: 9305919]
27. Wen Z, Zhong Z, Darnell JE Jr. Maximal activation of transcription by Stat1 and Stat3 requires both tyrosine and serine phosphorylation. Cell. 1995; 82:241–250. [PubMed: 7543024]
28. Arredondo J, Chernyavsky AI, Jolkovsky DL, Pinkerton KE, Grando SA. Receptor-mediated tobacco toxicity: cooperation of the Ras/Raf-1/MEK1/ERK and JAK-2/STAT-3 pathways

downstream of alpha7 nicotinic receptor in oral keratinocytes. FASEB J. 2006; 20:2093–2101. [PubMed: 17012261]

29. Chaturvedi P, Singh AP, Chakraborty S, Chauhan SC, Bafna S, Meza JL, et al. MUC4 mucin interacts with and stabilizes the HER2 oncoprotein in human pancreatic cancer cells. Cancer Res. 2008; 68:2065–2070. [PubMed: 18381409]
30. Provenzano PP, Keely PJ. The role of focal adhesion kinase in tumor initiation and progression. Cell Adh Migr. 2009; 3:347–350. [PubMed: 19690467]
31. Wong HP, Li ZJ, Shin VY, Tai EK, Wu WK, Yu L, et al. Effects of cigarette smoking and restraint stress on human colon tumor growth in mice. Digestion. 2009; 80:209–214. [PubMed: 19776585]
32. Majumdar AP, Davis GA, Dubick MA, Geokas MC. Nicotine stimulation of protein secretion from isolated rat pancreatic acini. Am J Physiol. 1985; 248:G158–G163. [PubMed: 2578743]
33. Rubin H. Selective clonal expansion and microenvironmental permissiveness in tobacco carcinogenesis. Oncogene. 2002; 21:7392–7411. [PubMed: 12379881]
34. Sheppard BJ, Williams M, Plummer HK, Schuller HM. Activation of voltage-operated Ca2+-channels in human small cell lung carcinoma by the tobacco-specific nitrosamine 4-(methylnitrosamino)-1-(3-pyridyl)-1-butanone. Int J Oncol. 2000; 16:513–518. [PubMed: 10675483]
35. Shen JX, Yakel JL. Nicotinic acetylcholine receptor-mediated calcium signaling in the nervous system. Acta Pharmacol Sin. 2009; 30:673–680. [PubMed: 19448647]
36. Plummer HK III, Dhar M, Schuller HM. Expression of the alpha7 nicotinic acetylcholine receptor in human lung cells. Respir Res. 2005; 6:29. [PubMed: 15807899]
37. Dasgupta P, Rastogi S, Pillai S, Ordonez-Ercan D, Morris M, Haura E, et al. Nicotine induces cell proliferation by beta-arrestin-mediated activation of Src and Rb-Raf-1 pathways. J Clin Invest. 2006; 116:2208–2217. [PubMed: 16862215]
38. Marrero MB, Bencherif M. Convergence of alpha 7 nicotinic acetylcholine receptor-activated pathways for anti-apoptosis and anti-inflammation: central role for JAK2 activation of STAT3 and NF-kappaB. Brain Res. 2009; 1256:1–7. [PubMed: 19063868]
39. Macha MA, Matta A, Chauhan SS, Siu KW, Ralhan R. Guggulsterone (GS) inhibits smokeless tobacco and nicotine-induced NF-kappaB and STAT3 pathways in head and neck cancer cells. Carcinogenesis. 2011; 32:368–380. [PubMed: 21177768]
40. Chen RJ, Ho YS, Guo HR, Wang YJ. Rapid activation of Stat3 and ERK1/2 by nicotine modulates cell proliferation in human bladder cancer cells. Toxicol Sci. 2008; 104:283–293. [PubMed: 18448488]
41. Chen RJ, Ho YS, Guo HR, Wang YJ. Long-term nicotine exposure-induced chemoresistance is mediated by activation of Stat3 and downregulation of ERK1/2 via nAChR and beta-adrenoceptors in human bladder cancer cells. Toxicol Sci. 2010; 115:118–130. [PubMed: 20106947]
42. Andoh A, Shioya M, Nishida A, Bamba S, Tsujikawa T, Kim-Mitsuyama S, et al. Expression of IL-24, an activator of the JAK1/STAT3/SOCS3 cascade, is enhanced in inflammatory bowel disease. J Immunol. 2009; 183:687–695. [PubMed: 19535621]
43. Mejias-Luque R, Peiro S, Vincent A, Van SI, de BC. IL-6 induces MUC4 expression through gp130/STAT3 pathway in gastric cancer cell lines. Biochim Biophys Acta. 2008; 1783:1728–1736. [PubMed: 18573283]
44. Mejias-Luque R, Linden SK, Garrido M, Tye H, Najdovska M, Jenkins BJ, et al. Inflammation modulates the expression of the intestinal mucins MUC2 and MUC4 in gastric tumors. Oncogene. 2010; 29:1753–1762. [PubMed: 20062084]
45. Arredondo J, Chernyavsky AI, Marubio LM, Beaudet AL, Jolkovsky DL, Pinkerton KE, et al. Receptor-mediated tobacco toxicity: regulation of gene expression through alpha3beta2 nicotinic receptor in oral epithelial cells. Am J Pathol. 2005; 166:597–613. [PubMed: 15681842]
46. Arredondo J, Chernyavsky AI, Grando SA. Nicotinic receptors mediate tumorigenic action of tobacco-derived nitrosamines on immortalized oral epithelial cells. Cancer Biol Ther. 2006; 5:511–517. [PubMed: 16582591]
47. Andrianifahanana M, Agrawal A, Singh AP, Moniaux N, Van SI, Aubert JP, et al. Synergistic induction of the MUC4 mucin gene by interferon-gamma and retinoic acid in human pancreatic

tumour cells involves a reprogramming of signalling pathways. Oncogene. 2005; 24:6143–6154. [PubMed: 16007204]

48. Andrianifahanana M, Singh AP, Nemos C, Ponnusamy MP, Moniaux N, Mehta PP, et al. IFN-gamma-induced expression of MUC4 in pancreatic cancer cells is mediated by STAT-1 upregulation: a novel mechanism for IFN-gamma response. Oncogene. 2007; 26:7251–7261. [PubMed: 17525742]
49. Ponnusamy MP, Singh AP, Jain M, Chakraborty S, Moniaux N, Batra SK. MUC4 activates HER2 signalling and enhances the motility of human ovarian cancer cells. Br J Cancer. 2008; 99:520–526. [PubMed: 18665193]
50. Avizienyte E, Frame MC. Src and FAK signalling controls adhesion fate and the epithelial-to-mesenchymal transition. Curr Opin Cell Biol. 2005; 17:542–547. [PubMed: 16099634]
51. Vadlamudi RK, Sahin AA, Adam L, Wang RA, Kumar R. Heregulin and HER2 signaling selectively activates c-Src phosphorylation at tyrosine 215. FEBS Lett. 2003; 543:76–80. [PubMed: 12753909]

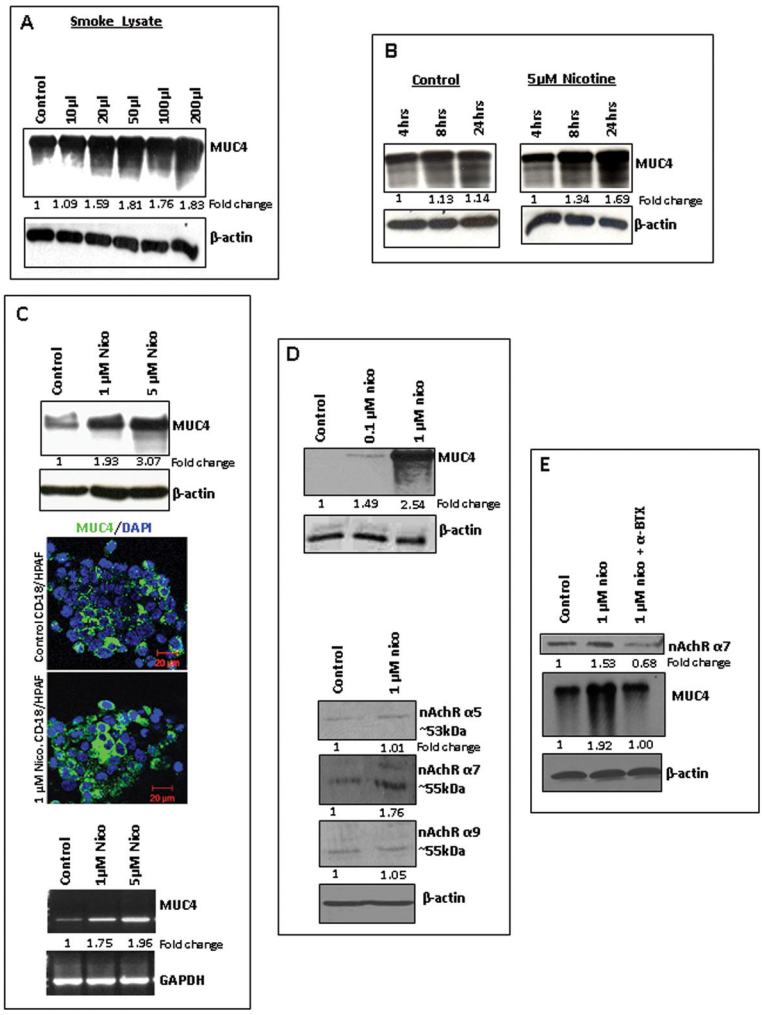

Figure 1.

Cigarette-smoke and nicotine-mediated MUC4 up-regulation and overexpression of the α7 nicotine receptor subunit in PC cells. **1*A***. CD18/HPAF cells were treated with different doses of cigarette-smoke extract (CSE) (10µl-200µl) for 24hrs; the untreated cells were kept as mock control. Western blot analysis, using the mouse anti-MUC4 mAb (8G7, generated in our laboratory), showed a progressive increase in the MUC4 expression with CSE. ***1B.*** CD18/HPAF cells were treated with 5µM nicotine for different time points (4hrs, 8hrs and 24hrs). Nicotine treatment increased the MUC4 expression in a time-dependent manner with a maximum expression at 24hrs after the treatment. ***1C.*** Nicotine increased the MUC4 expression levels in CD18/HPAF cells in a dose-dependent manner as seen by the Western blot analysis and RT PCR analysis, β-actin and GAPDH were used as internal controls. Confocal immunofluorescence also showed an increased MUC4 expression (FITC: green) in the nicotine-treated CD18/HPAF cells as compared to the untreated cells. ***1D.*** Nicotine induced MUC4 expression in CD18/HPAF-SF cells with 0.1µM dose of nicotine which progressively increased with 1µM dose treatment of nicotine. The Western blot analysis showed a significant stimulation of the α7nAChR subunit with nicotine treatment (1µM), whereas, there was no change in the expression levels of the other nAchR subunits such as

α9 and α5. ***1E.*** The 1μM nicotine treatments lead to the stimulation of the α7nAChR subunit in CD18/HPAF cells. Treatment of the CD18/HPAF cells with the α7 nicotine receptor subunit antagonist, α-bungarotoxin (α-BTX) (1μM) resulted in down-regulation of the expression levels of α7nAChR subunit and nicotine-induced MUC4. β-actin was used as an internal control. Western blots were quantified using the software ChemiImager4400. The numerical values specified beneath the respective bands of Western blots represent the fold change in protein expression as compared to that of the control (1.0).

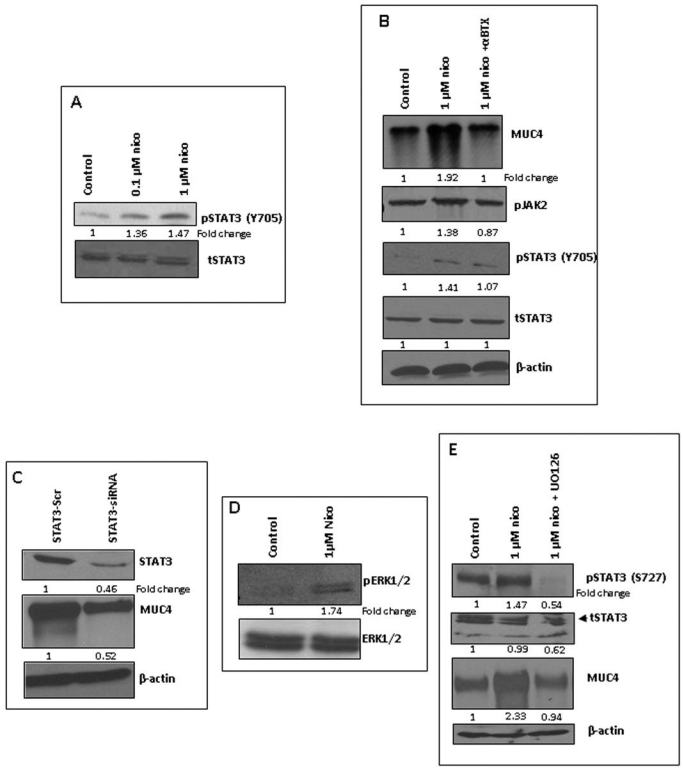

Figure 2.

α7nAChR subunit-mediated activation of the JAK2-STAT3 pathway in PC cells. ***2A.*** Western blot analysis showed that nicotine increases the expression of pSTAT3 (Y705) in CD18/HPAF-SF cells in a dose-dependent manner (0.1μM, 1μM). ***2B***. The 1μM nicotine treatment increased the MUC4, pJAK2 and pSTAT3 (Y705) expression levels which were abrogated upon α-BTX treatment in CD18/HPAF cells, while the total STAT3 expression levels remained unchanged. **2*C.*** The siSTAT3-mediated knockdown of STAT3 in CD18/HPAF cells showed a down-regulation of nicotine-induced MUC4 expression along with the reduced STAT3 expression levels as compared to the scramble oligo's-transfected cells ***2D.*** The 1μM nicotine treatment of CD18/HPAF cells showed an increased ERK activation as compared to the untreated cells. The total ERK expression levels remained unchanged. ***2E.*** Treatment of the CD18/HPAF cells with an ERK1/2 inhibitor, U0126 (1μM), resulted in reduced expression levels of nicotine-induced MUC4 and pSTAT3 (S727), as well as demonstrated a decrease in tSTAT3 expression. The pJAK2 and pSTAT3 stimulation was monitored after 24hrs of treatment, however pERK stimulation was monitored after 1hr of treatment. Western blots were quantified using the software, ChemiImager4400. The numerical values specified beneath the respective bands of Western blots represent the fold change in protein expression as compared to that of the control (1.0).

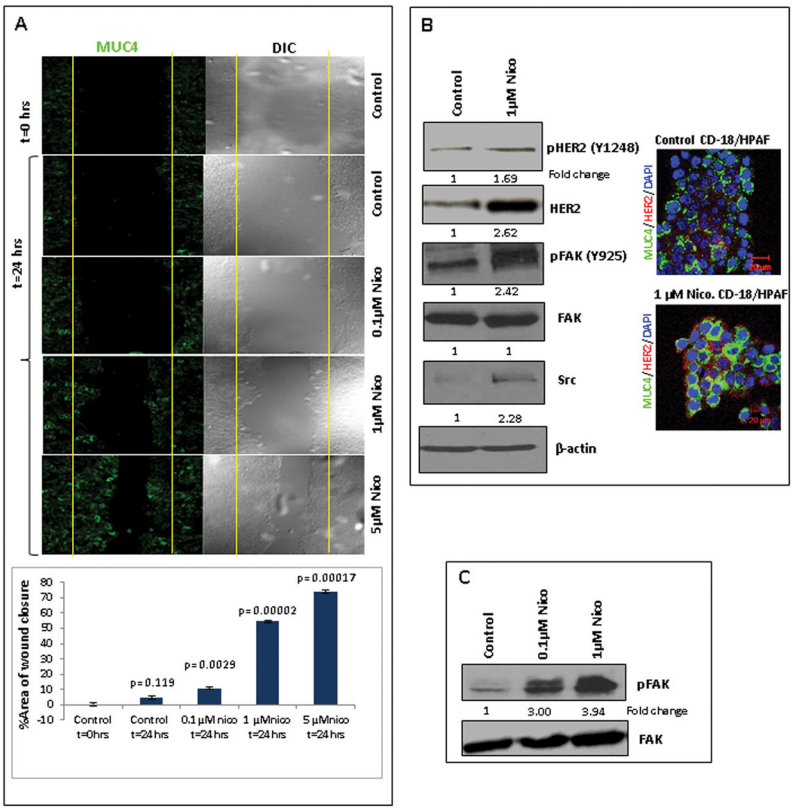

Figure 3.

Nicotine-mediated increased migratory potential of the PC cells, increased levels of tHER2 and c-Src and enhanced activation of HER2 and FAK. ***3A.*** CD18/HPAF cells were seeded on cover slips and were treated with different doses of nicotine for 24 hrs. On the same cover slips, the wound healing assay was also performed. The confocal analysis showed a progressive increase in the MUC4 expression (FITC: green) with nicotine treatment. The wound healing assay showed a progressive increase in the migration potential of the CD18/HPAF cells in a dose-dependent manner (0.1μM, 1μM, 5μM of nicotine) as compared to the untreated cells. The migration of cells toward the wounds was expressed as percentage of wound closure: % of wound closure= $[(A_{t=0hrs} - A_{t=\Delta hrs})/ A_{t=0hrs})] * 100\%$, where, $A_{t=0hrs}$ is the initial area of wound measured immediately after scratching, and $A_{t=\Delta hrs}$ is the area of wound measured 24 hrs after scratching. Each experiment was performed at least 3 times. The Student *t*-test was employed for statistical analysis. Statistical significance was established at $p < 0.05$. ***3B.*** Western blot analysis showed an enhanced expression of total-HER2 in the nicotine-treated CD18/HPAF cells as compared to the untreated cells. Confocal immunofluorescence also showed an increased expression of total-HER2 (Texas red: Red) and enhanced co-localization with MUC4 (FITC: Green) in the nicotine-treated cells as compared to the control cells. Western blot analysis showed that nicotine treatment potentiates the HER2 and FAK activation and increases the levels of c-Src. β-actin was used as an internal control. ***3C.*** Western blot analysis showed that nicotine treatment increased the phosphorylation of FAK in the CD18/HPAF-SF cells in a dose-dependent manner (0.1μM, 1μM of nicotine). The total FAK expression remained unaltered. Western blots

were quantified using the software, ChemiImager4400. The numerical values specified beneath the respective bands of Western blots represent the fold change in protein expression as compared to that of the control (1.0).

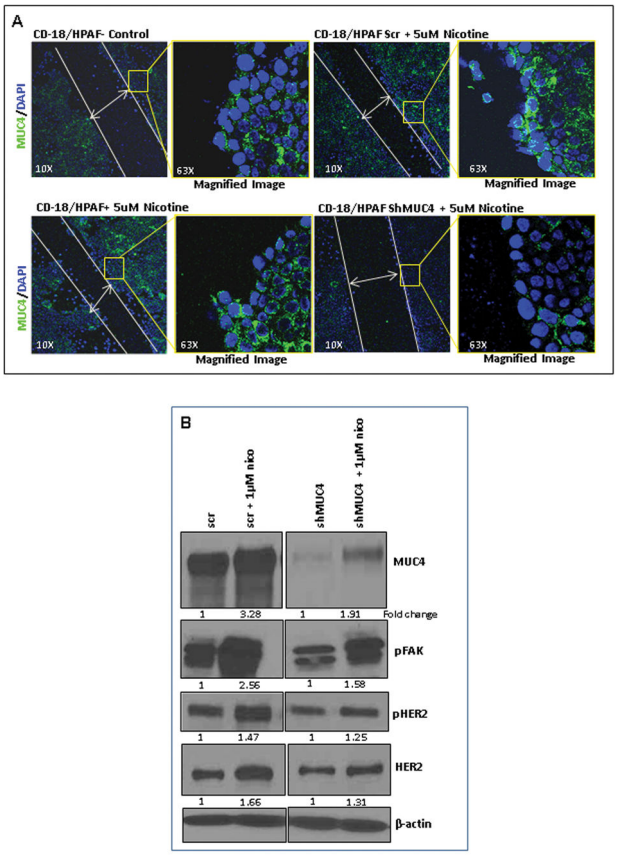

Figure 4.

Nicotine-mediated effects are MUC4-dependent. ***4A.*** The wound healing assay was performed using the shMUC4 and scr-Vector transfected CD18/HPAF cells under nicotine treatment. In parallel, the confocal analysis was carried out. The scr-vector transfected CD18/HPAF cells showed an increase in the migration potential upon nicotine treatment, however, no variation was observed both with the untreated and nicotine-treated shMUC4 transfected cells. The left panel is the lower magnification (10X) image showing the closure of the wound by the migrating PC cells. The panel on the right is higher magnification (63X) image of the area on the edge of the wound (square box) demonstrating MUC4 expression (FITC: Green) in the cells. ***4B.*** The downstream effectors of MUC4 (FAK, HER2) responsible for the increased metastatic potential of the PC cells were investigated in MUC4 knockdown PC cells. In CD18/HPAF/scr cells, 1μM nicotine treatment induced high levels of MUC4 leading to an increased expression of HER2, pHER2 and pFAK as compared to CD18/HPAF/shMUC4 cells. β-actin was used as an internal control. Western blots were quantified using the software, ChemiImager4400. The numerical values specified beneath the respective bands of Western blots represent the fold change in protein expression as compared to that of the control (1.0).

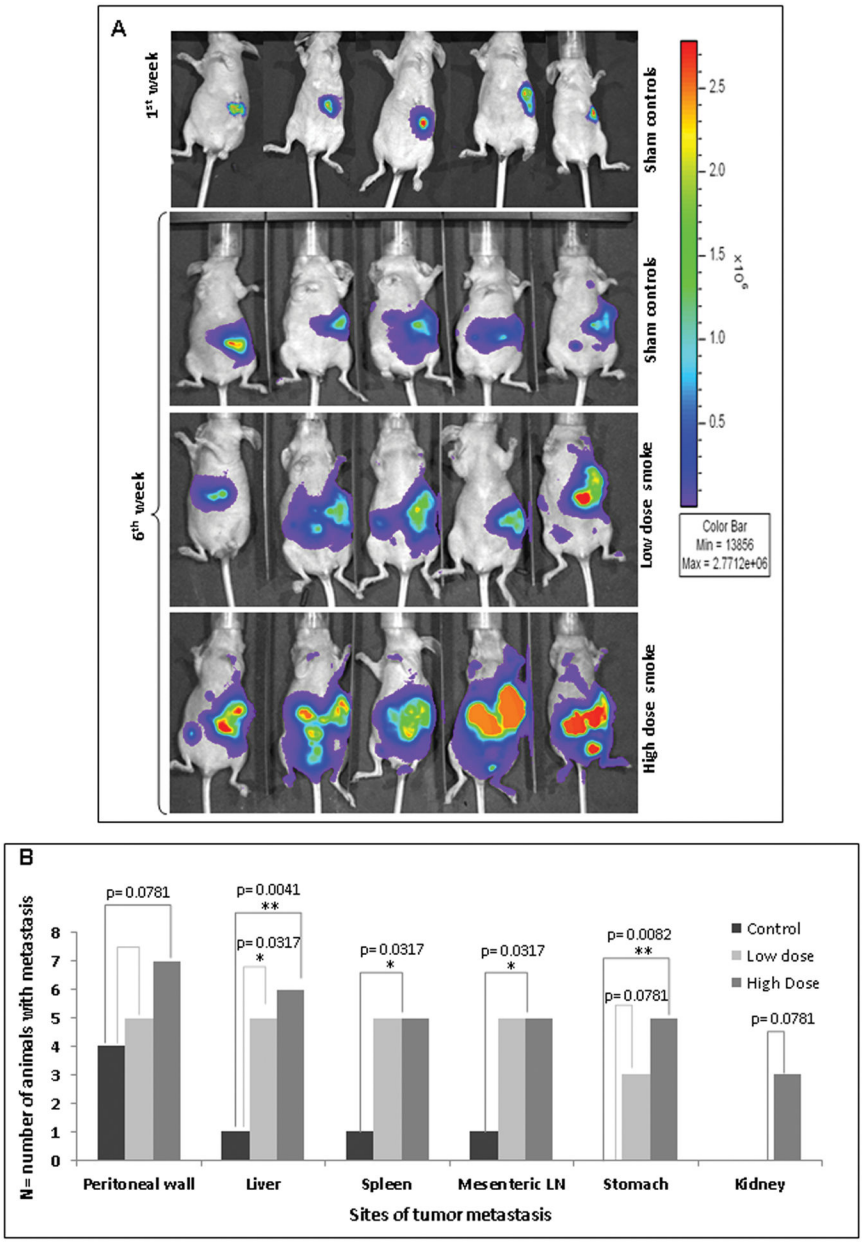

Figure 5.

Cigarette-smoke-mediated increase in pancreatic tumor metastasis ***5A.*** Immunodefficient mice were orthotopically implanted with luciferase-containing CD18/HPAF cells and routinely exposed to an average of 100mg/m^3 TSP for the low-dose and 247mg/m^3 TSP for the high-dose of cigarette-smoke, for six weeks. The Representative *in vivo* bioluminescent imaging of the CS-exposed mice showed an increased tumor size as compared to the sham controls and a significant increase in the metastasis in both the low-dose-exposed animals and high-dose-exposed animals as compared to the sham controls. All the images are normalized to the same scale. ***5B.*** Statistical analysis showed significant tumor metastasis to various potential organ sites, including the peritoneal wall, liver, spleen, mesenteric lymph

nodes, stomach and kidney. P-values lower than 0.05 were considered statistically significant (*).

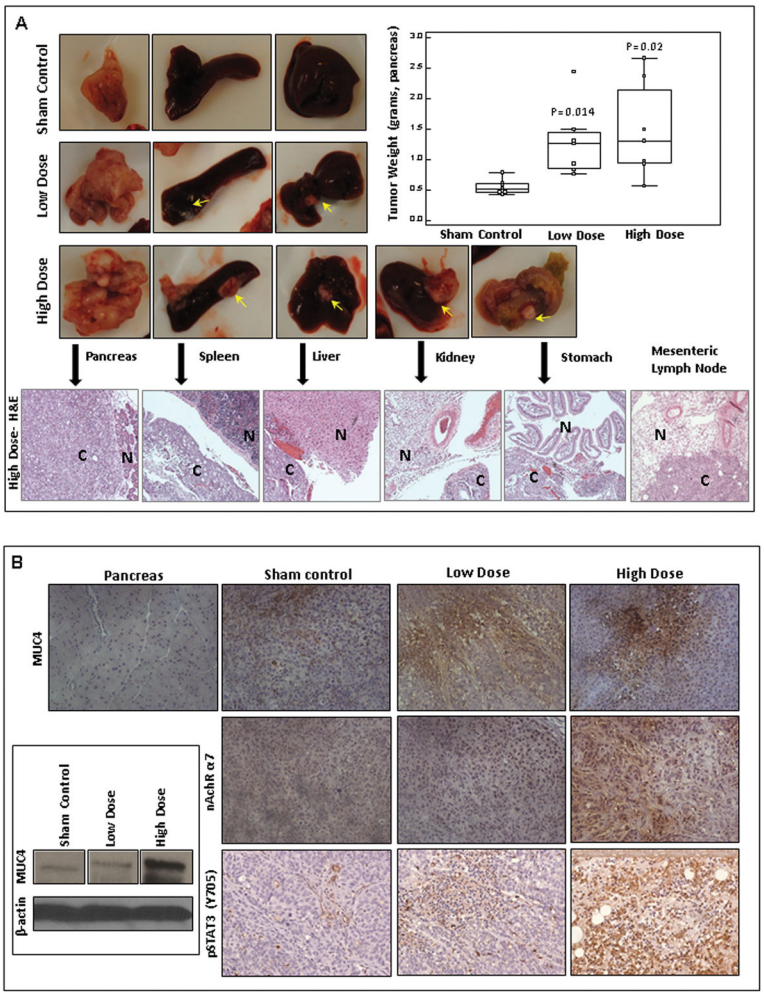

Figure 6.

Cigarette-smoke-mediated increase in the tumor size and expression levels of MUC4, α7nAChR subunit and pSTAT3. ***6A.*** The macroscopic examinations of the pancreas and the distant organs with pancreatic tumor metastasis showing that CS-exposure significantly increased the tumor metastasis to spleen and liver both in low-dose-exposed and high-dose-exposed mice groups as compared to the sham controls. The high-dose-exposed group showed significant number of metastatic nodules also in the kidney and stomach (arrows point to the metastatic nodules). Box-and-Whisker plot shows the increase in the mean pancreatic tumor weight in a dose-dependent manner upon CS-exposure as compared to the sham controls. P-values lower than 0.05 were considered statistically significant. The H&E staining of organs showed the histopathological aberrations in the metastatic cancer tissues (C) as compared to the normal tissues (N). ***6B.*** Immunohistochemistry (8G7; 1:2500) and Western blotting analysis (8G7; 1:2000) showed that cigarette-smoke progressively increases the MUC4 expression levels in a dose-dependent manner as compared to the sham controls. Immunohistochemistry revealed that the expression levels of α7nAChR subunit and pSTAT3 were enhanced in the CS-exposed mice as compared to the sham controls.

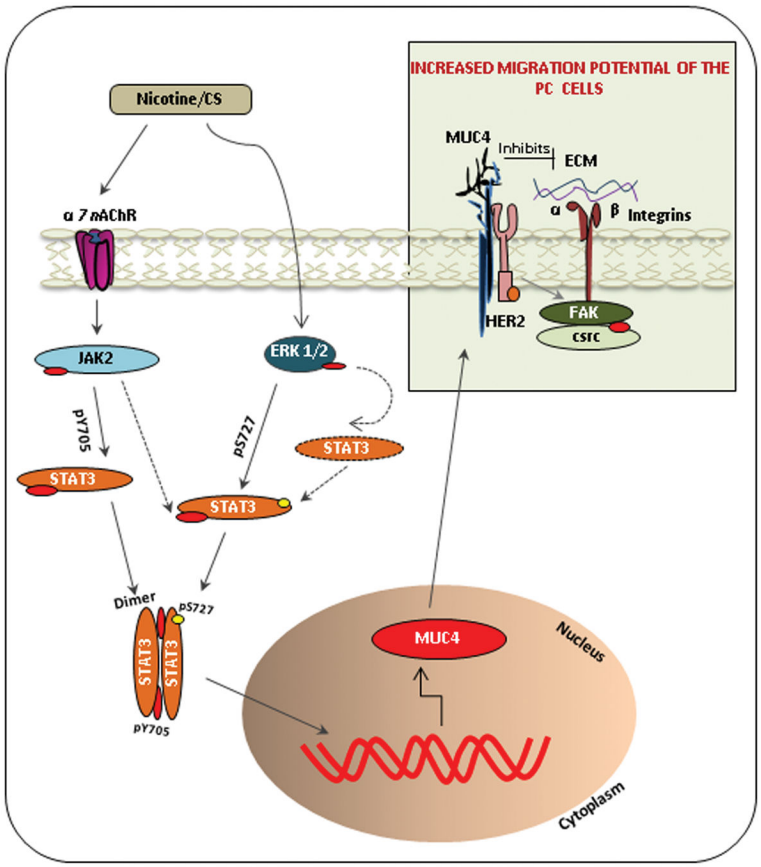

Figure 7.

Nicotine-induced α7nAChR/JAK2 pathway in cooperation with nicotine-mediated ERK1/2 activation potentiates STAT3 activation in PC cells. The ERK1/2-mediated STAT3 phosphorylation (pS727) is known to enhance the DNA binding as well as to stabilize the cytoplasmic STAT3 levels. Whereas, the phosphorylated STAT3 (Y705) forms a dimer and translocate into the nucleus where it plays the key role in the up-regulation of MUC4 mucin expression. The transmembrane MUC4 mucin, upon expression on the membrane of the cells, causes an alteration in the migratory potential of PC cells. MUC4, being a large sized protein, could be speculated to either directly inhibit the interaction between the integrin and the extra cellular matrix (ECM) by stearic hindrance, or it could alter the downstream signaling pathways mediated by HER2 and c-Src activation, resulting in the activation of integrin and FAK signaling. This leads to the suppression of cell–cell adhesion, thereby causing an increase in the migratory potential of PC cells. Altogether, these events result in cancer cell spread and hence contribute to metastasis of pancreatic cancer.